Supporting Information

Size-dependent Abnormal Thermo-enhanced Luminescence of Ytterbium Doped Nanoparticles

Xiangshui Cui[ab], Yao Cheng*[a], Hang Lin [a], Feng Huang [a] and Yuansheng Wang*[a]

[a] Key Laboratory of Design and Assembly of Functional Nanostructures, Fujian Institute of Research on the Structure of Matter, Chinese Academy of Sciences, Fuzhou, Fujian, 350002, P. R. China.

[b] University of Chinese Academy of Sciences, Beijing, 100049, P. R. China.

* Corresponding authors. E-mail addresses: chengyao@fjirsm.ac.cn; yswang@fjirsm.ac.cn.

Supporting Figures

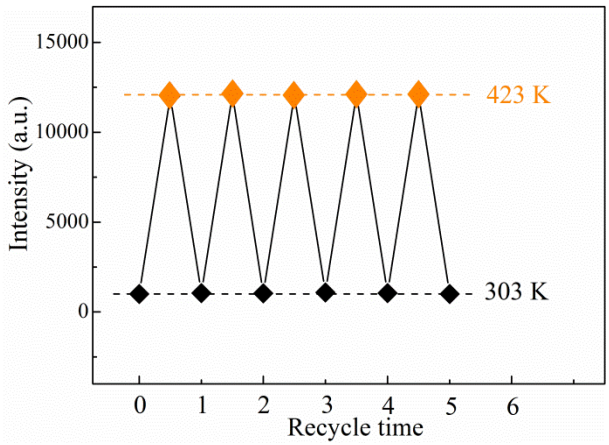

Figure S1. Cycle mesurements of abnormal thermo-enhanced UCL of $NaGdF_4:Yb^{3+}/Eu^{3+}$ (20/10 mol %) LNPs with size of 10 nm.

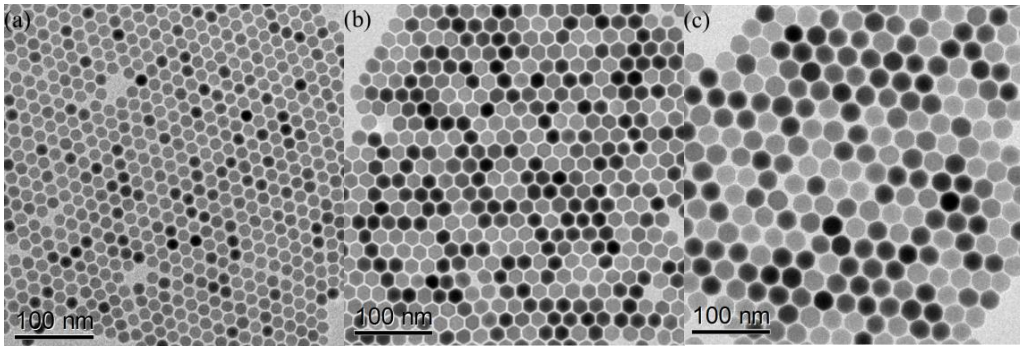

Figure S2. TEM micrographs of the $NaGdF_4$: Yb^{3+}/Eu^{3+} (20/10 mol %) LNPs with different sizes of (a) 15 nm, (b) 20 nm, and (c) 25 nm.

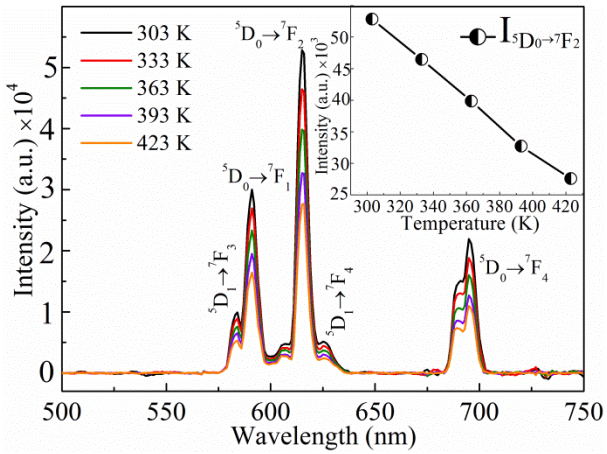

Figure S3. Temperature-dependent UCL emission spectra (λ_{ex}=980 nm) of the bulk (>50 nm) $NaGdF_4$:Yb^{3+}/Eu^{3+} (20/10 mol %) materials.

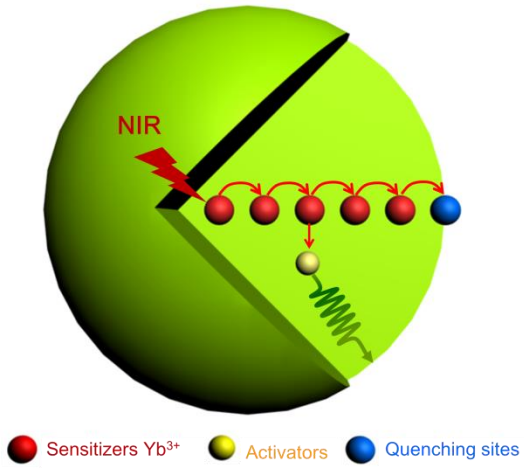

Figure S4. Schematic diagram of surface quenching based on the Yb^{3+}-mediated energy migration.

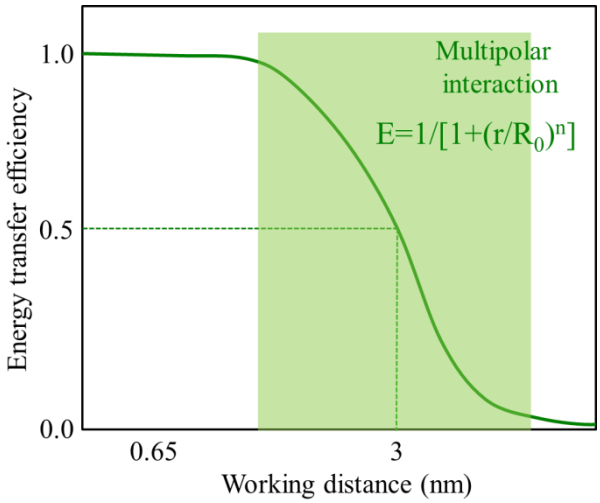

Figure S5. Schematic showing the influence of working distance on nonradiative energy transfer (multipolar interaction) efficiency. [S1, S2,S3]

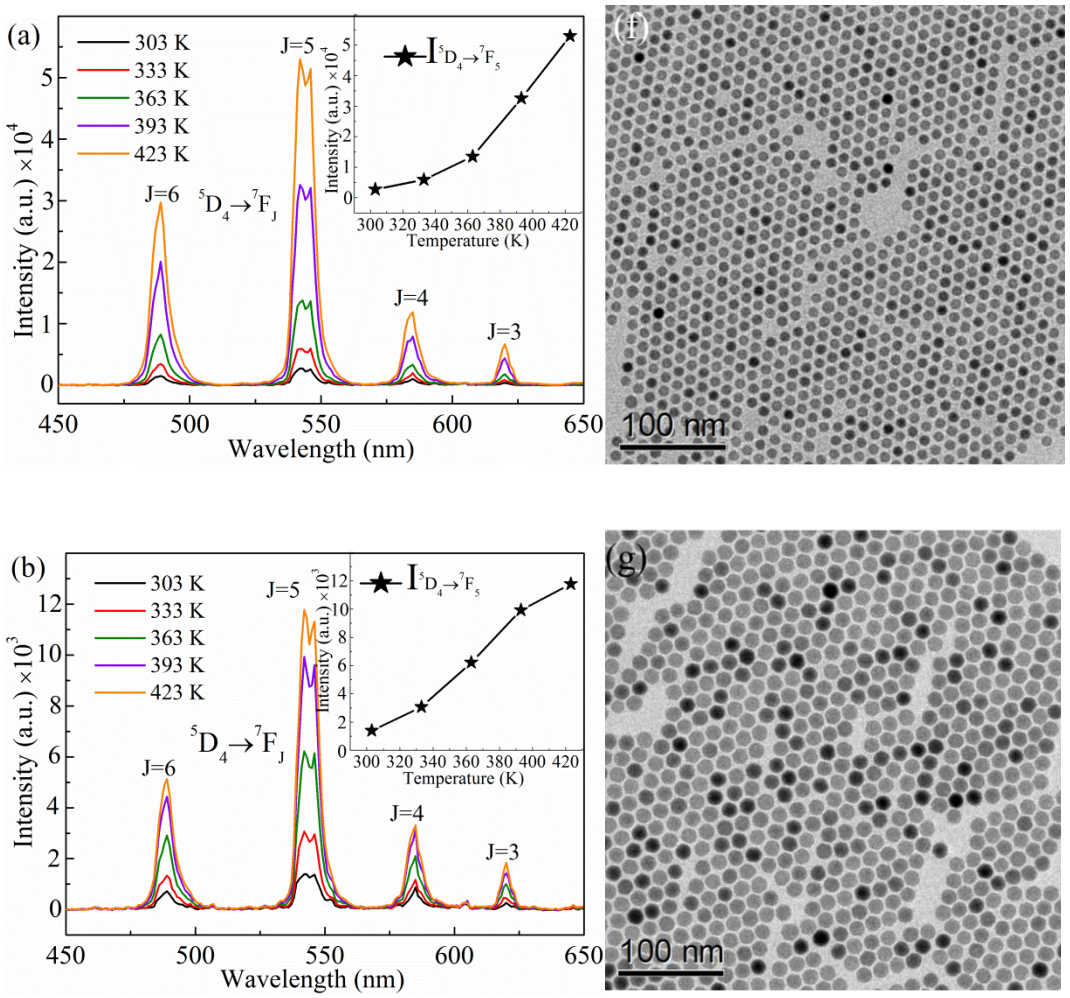

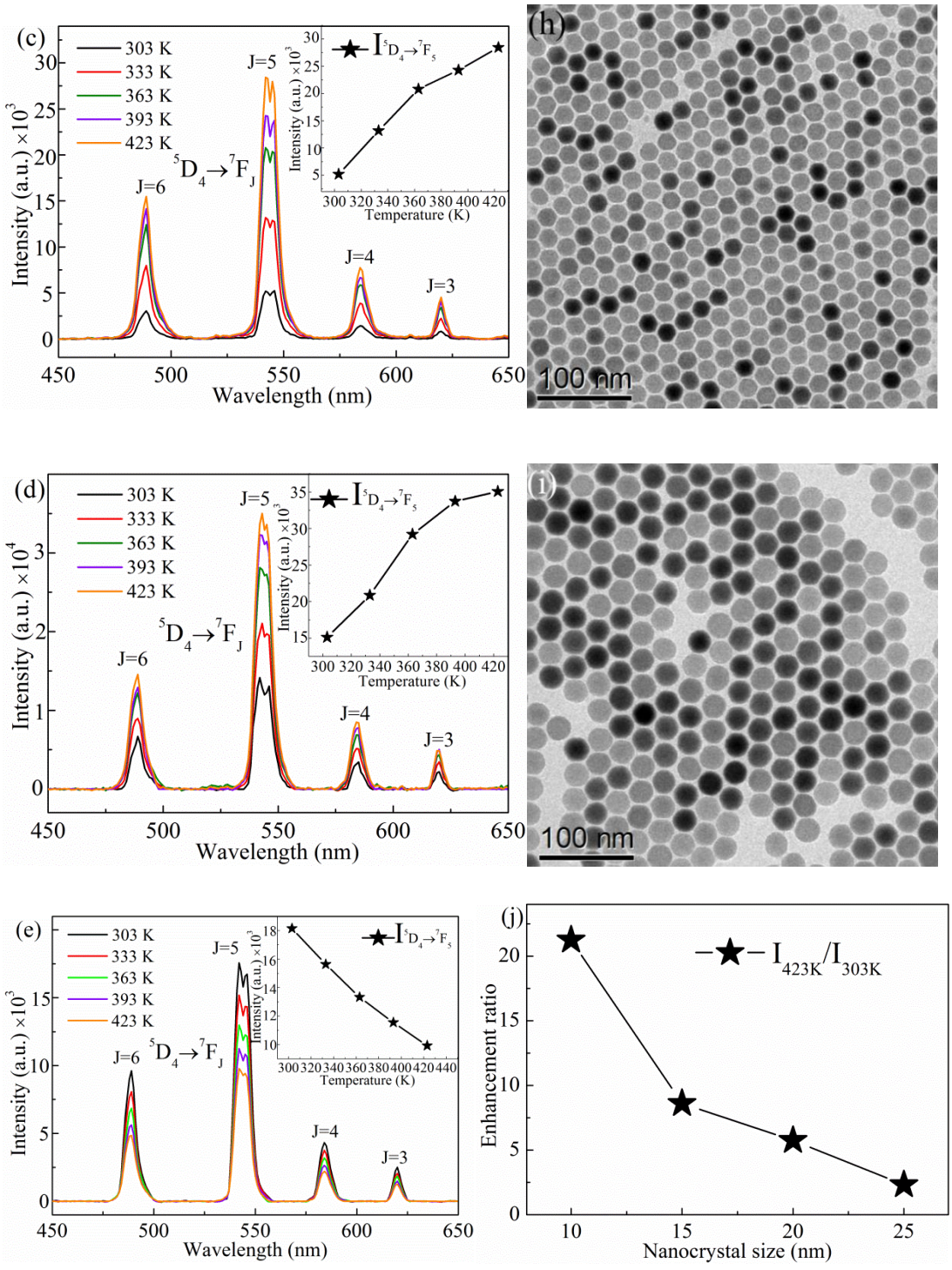

Figure S6. Temperature-dependent UCL emission spectra (λ_{ex}=980 nm) of (a) 10 nm, (b) 15 nm, (c) 20 nm, (d) 25 nm, and (e) bulk $NaGdF_4$: Yb^{3+}/Tb^{3+} (20/10 mol%) samples; (f-i) the corresponding TEM micrographs of the a-d samples. (j) Line chart of the integrated intensity ratio for the $^5D_4 \rightarrow {}^7F_5$ transition (I_{423K}/I_{303K}) against the nanocrystal size.

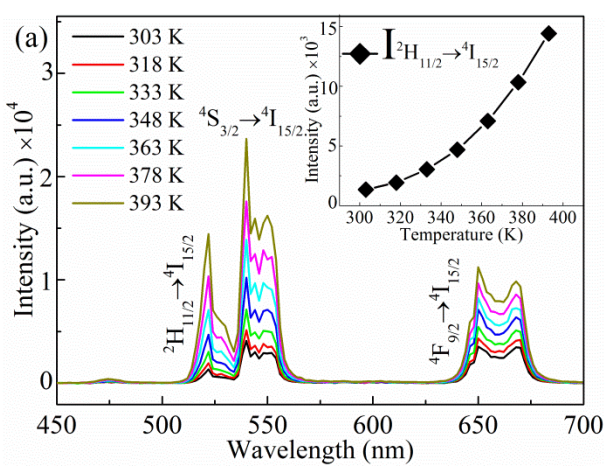
(a)
303 K
318 K
333 K
348 K
363 K
378 K
393 K
$^4S_{3/2}\rightarrow{}^4I_{15/2}$
$^2H_{11/2}\rightarrow{}^4I_{15/2}$
$^4F_{9/2}\rightarrow{}^4I_{15/2}$
$I_{^2H_{11/2}\rightarrow{}^4I_{15/2}}$
Intensity (a.u.) ×10^3
Temperature (K)
Intensity (a.u.) ×10^4
Wavelength (nm)

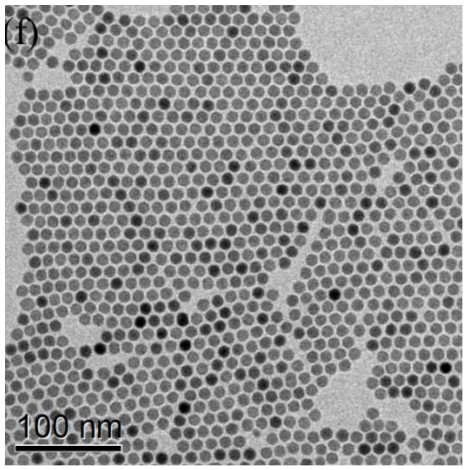
(f)
100 nm

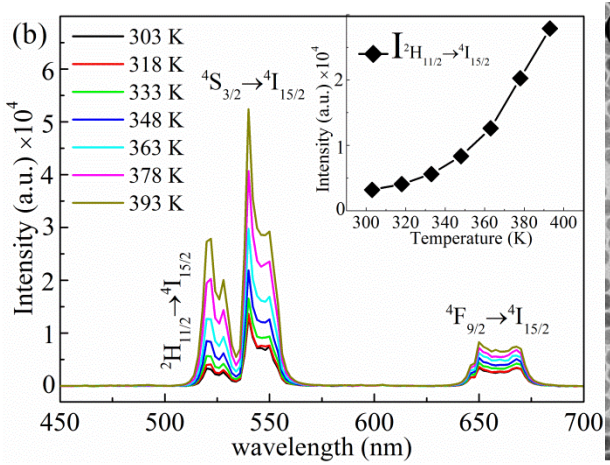
(b)
303 K
318 K
333 K
348 K
363 K
378 K
393 K
$^4S_{3/2}\rightarrow{}^4I_{15/2}$
$^2H_{11/2}\rightarrow{}^4I_{15/2}$
$^4F_{9/2}\rightarrow{}^4I_{15/2}$
$I_{^2H_{11/2}\rightarrow{}^4I_{15/2}}$
Intensity (a.u.) ×10^4
Temperature (K)
Intensity (a.u.) ×10^4
wavelength (nm)

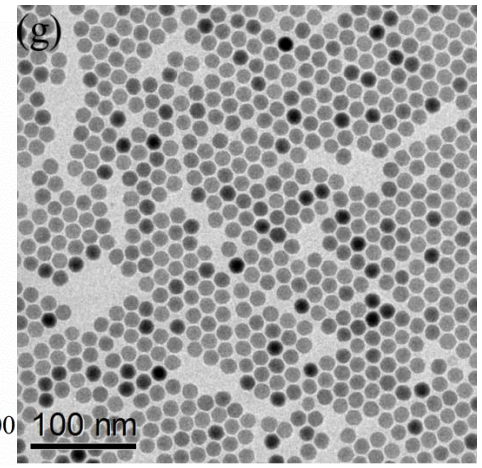
(g)
100 nm

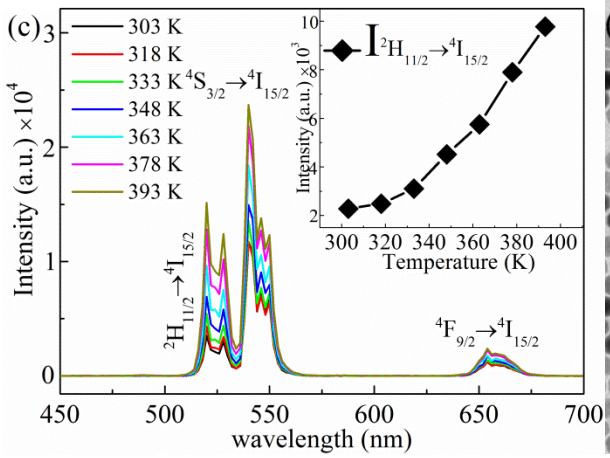
(c)
303 K
318 K
333 K
348 K
363 K
378 K
393 K
$^4S_{3/2}\rightarrow{}^4I_{15/2}$
$^2H_{11/2}\rightarrow{}^4I_{15/2}$
$^4F_{9/2}\rightarrow{}^4I_{15/2}$
$I_{^2H_{11/2}\rightarrow{}^4I_{15/2}}$
Intensity (a.u.) ×10^3
Temperature (K)
Intensity (a.u.) ×10^4
wavelength (nm)

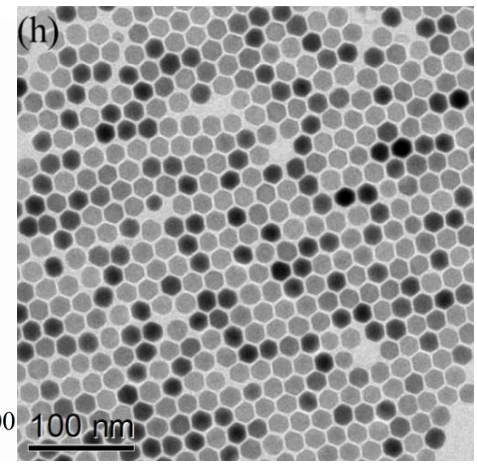
(h)
100 nm

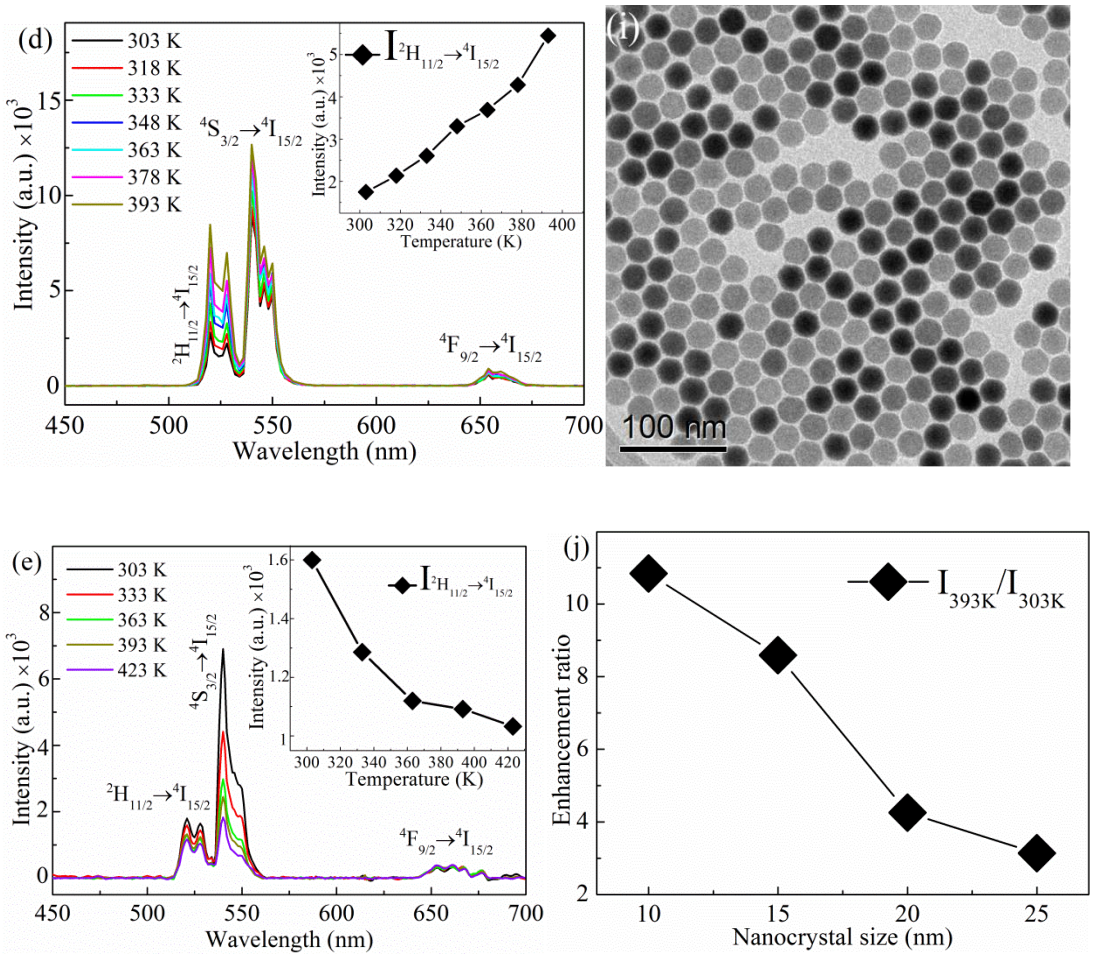

Figure S7. Temperature-dependent UCL emission spectra (λ_{ex}=980 nm) of (a) 10 nm, (b) 15 nm, (c) 20 nm, (d) 25 nm, and (e) bulk $NaGdF_4:Yb^{3+}/Er^{3+}$ (20/0.5 mol%) samples; (f-i) the corresponding TEM micrographs of the a-d samples. (j) Line chart of the integrated intensity ratio for the $^2H_{11/2}\rightarrow{}^4I_{15/2}$ transition (I_{393K}/I_{303K}) against the nanocrystal size.

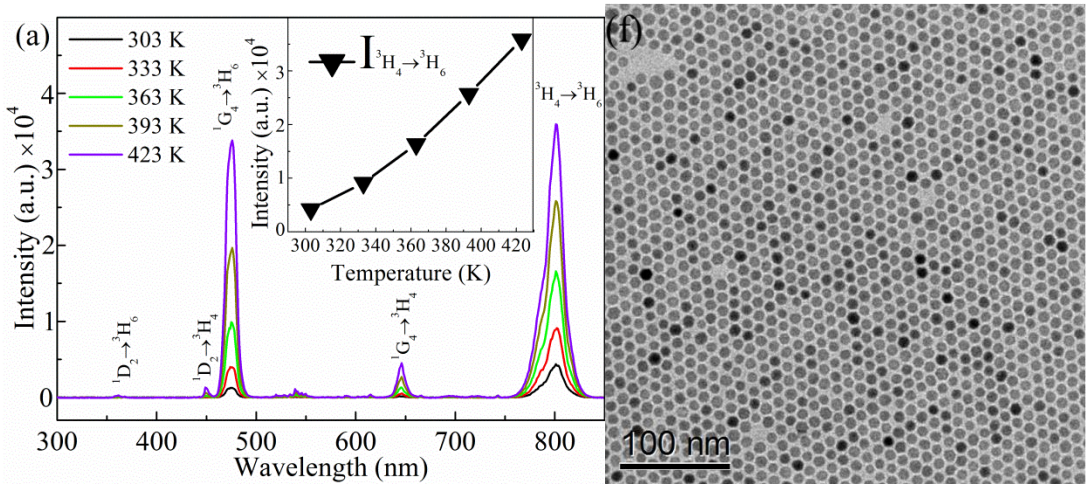

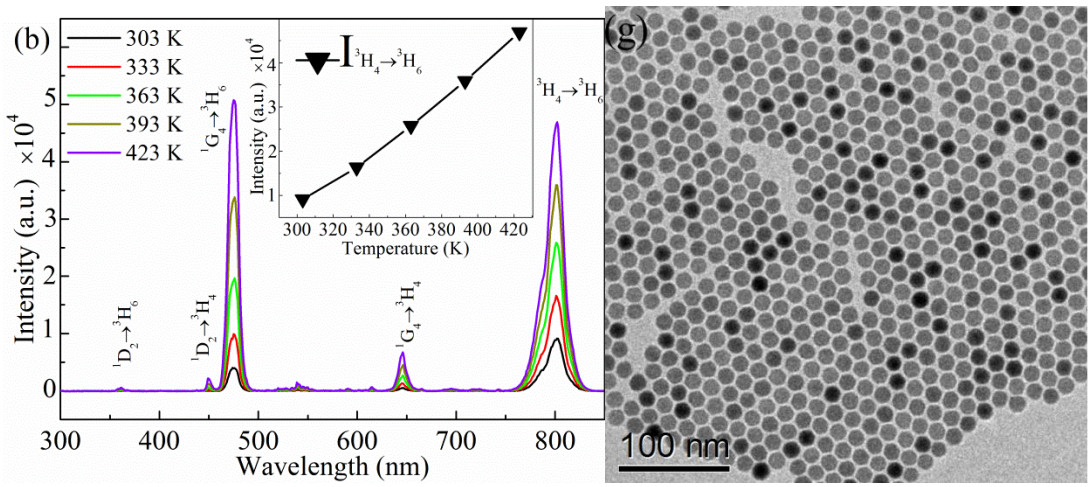
(b)
303 K
333 K
363 K
393 K
423 K
Intensity (a.u.) ×10^4
Wavelength (nm)
$^1D_2 \rightarrow {}^3H_6$
$^1D_2 \rightarrow {}^3H_4$
$^1G_4 \rightarrow {}^3H_6$
$^1G_4 \rightarrow {}^3H_4$
$^3H_4 \rightarrow {}^3H_6$
$I_{^3H_4 \rightarrow {}^3H_6}$
Intensity (a.u.) ×10^4
Temperature (K)
(g)
100 nm

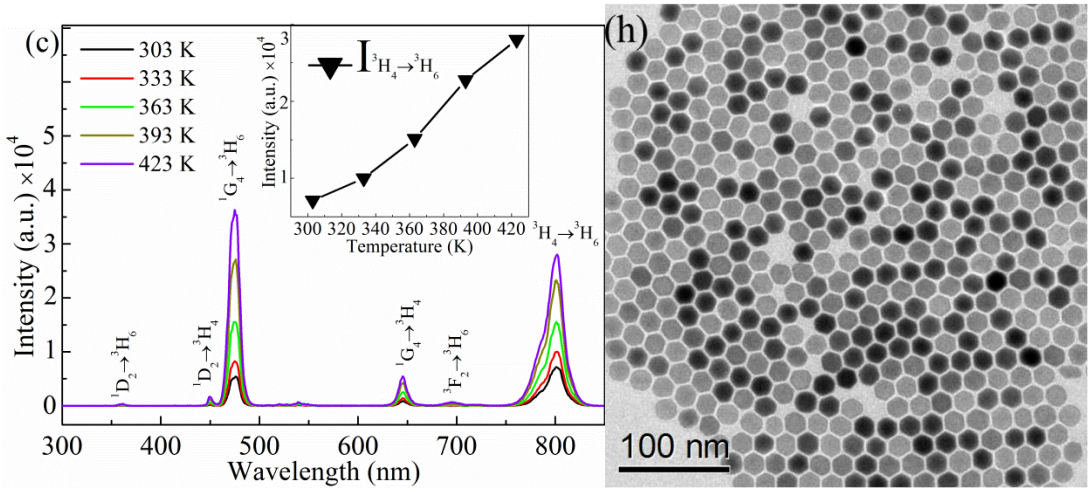
(c)
303 K
333 K
363 K
393 K
423 K
Intensity (a.u.) ×10^4
Wavelength (nm)
$^1D_2 \rightarrow {}^3H_6$
$^1D_2 \rightarrow {}^3H_4$
$^1G_4 \rightarrow {}^3H_6$
$^1G_4 \rightarrow {}^3H_4$
$^3F_2 \rightarrow {}^3H_6$
$^3H_4 \rightarrow {}^3H_6$
$I_{^3H_4 \rightarrow {}^3H_6}$
Intensity (a.u.) ×10^4
Temperature (K)
(h)
100 nm

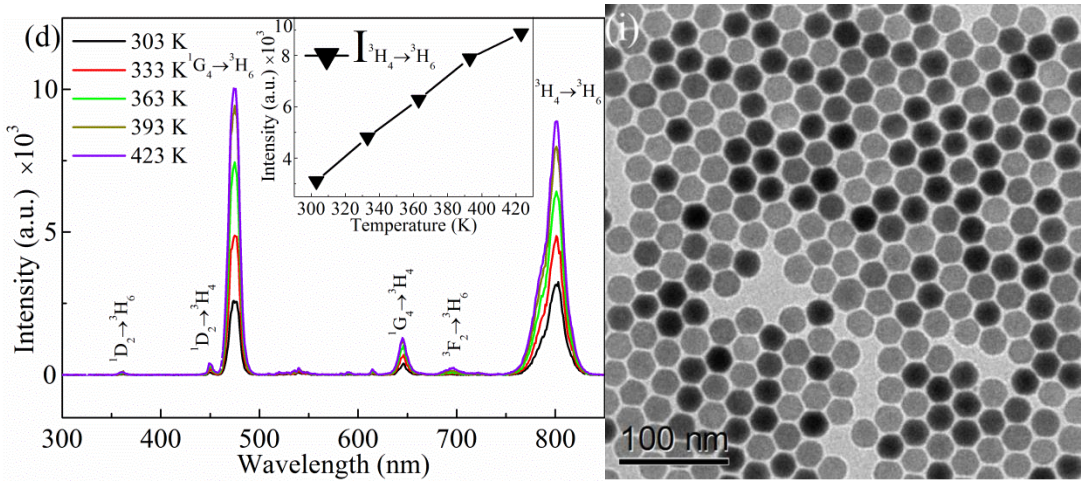
(d)
303 K
333 K
363 K
393 K
423 K
Intensity (a.u.) ×10^3
Wavelength (nm)
$^1D_2 \rightarrow {}^3H_6$
$^1D_2 \rightarrow {}^3H_4$
$^1G_4 \rightarrow {}^3H_6$
$^1G_4 \rightarrow {}^3H_4$
$^3F_2 \rightarrow {}^3H_6$
$^3H_4 \rightarrow {}^3H_6$
$I_{^3H_4 \rightarrow {}^3H_6}$
Intensity (a.u.) ×10^3
Temperature (K)
(i)
100 nm

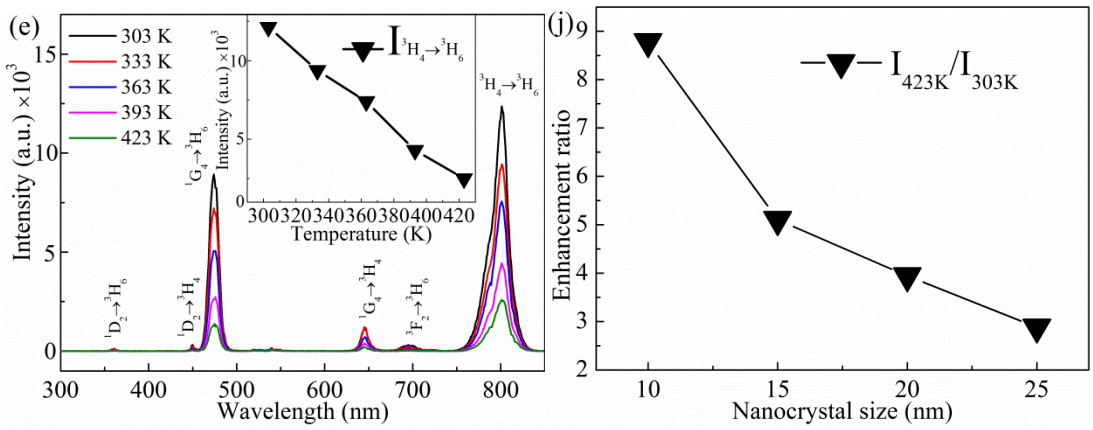

Figure S8. Temperature-dependent UCL emission spectra (λ_{ex}=980 nm) of (a) 10 nm, (b) 15 nm, (c) 20 nm, (d) 25 nm, and (e) bulk $NaGdF_4:Yb^{3+}/Tm^{3+}$ (20/0.2 mol%) samples; (f-i) the corresponding TEM micrograph of the a-d samples. (j) Line chart of the integrated intensity ratio for the $^3H_4 \rightarrow {}^3H_6$ transition (I_{423K}/I_{303K}) against the nanocrystal size.

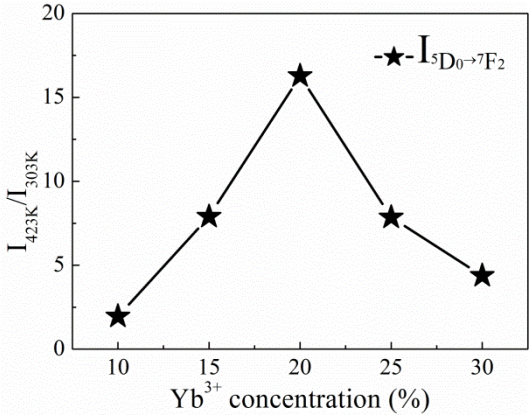

Figure S9. Plot of the intensity enhancement ratio of $^5D_0 \rightarrow {}^7F_2$ transition (I_{423K}/I_{303K}) against Yb^{3+} doping concentration for the $NaGdF_4:xYb^{3+}/10Eu^{3+}$ (x=10, 15, 20, 25, 30 mol%) LNPs with size of 10 nm.

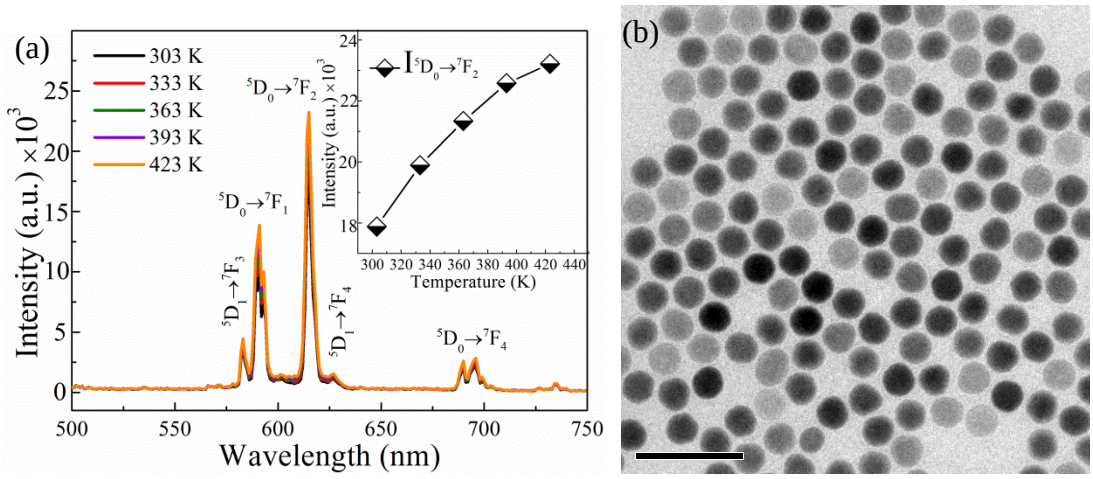

Figure S10. Temperature-dependent UCL emission spectra (λ_{ex}=980 nm) of core-shell $NaGdF_4$:Yb^{3+}/Eu^{3+}@$NaYF_4$ LNPs with the core size of 10 nm (a); and the corresponding TEM micrographs (b).

References

(S1) X. Chen, D. Peng, Q. Ju, F. Wang, *Chem. Soc. Rev.,* 2015**, 44**, 1318-1330.

(S2) X. Liu, J. R. Qiu, *Chem. Soc. Rev.,* 2015**, 44**, 8714-8746.

(S3) T. Ha, Th. Enderle, D. Ogletree, D. Chemla, P. Selvin, S. Weiss, *Proc. Natl. Acad. Sci.,* 1996**, 93**, 6264-6268.